Jüttner *et al. J Cardiovasc Aging* 2024;4:20
DOI: 10.20517/jca.2024.10

The Journal of Cardiovascular Aging

Original Research Article

Open Access

The modified 6-chromanol SUL-238 protects against accelerated vascular aging in vascular smooth muscle *Ercc1*-deficient mice

Annika A. Jüttner[1], Soroush Mohammadi Jouabadi[1], Janette van der Linden[1,2], Rene de Vries[1], Sander Barnhoorn[2], Ingrid M. Garrelds[1], Yoëlle Goos[1,3], Richard van Veghel[1], Ingrid van der Pluijm[2,4], A. H. Jan Danser[1], Pier G. Mastroberardino[2,5,6], Adrianus C. van der Graaf[7], Daniël H. Swart[7,8], Robert H. Henning[8], Jenny A. Visser[9], Guido Krenning[7,8], Anton J. M. Roks[1]

[1]Department of Internal Medicine, Erasmus MC, University Medical Center Rotterdam, Rotterdam 3015 GD, the Netherlands.
[2]Department of Molecular Genetics, Erasmus MC, University Medical Center Rotterdam, Rotterdam 3015 GD, the Netherlands.
[3]Department of Internal Medicine, Erasmus MC, University Medical Center, Rotterdam 3015 GD, the Netherlands.
[4]Department of Vascular Surgery, Cardiovascular Institute, Erasmus University Medical Center, Rotterdam 3015 GD, the Netherlands.
[5]IFOM-ETS, the AIRC Institute for molecular Oncology, Milan 20139, Italy.
[6]Università degli Studi dell'Aquila, L'Aquila 67100, Italy.
[7]Sulfateq B.V., Groningen 9726 GN, the Netherlands.
[8]Department of Clinical Pharmacy and Pharmacology, University Medical Centre Groningen, University of Groningen, Groningen 9713 AV, the Netherlands.
[9]Department of Internal Medicine, Erasmus MC, University Medical Center Rotterdam, Rotterdam 3015 GD, the Netherlands.

Correspondence to: Dr. Anton J. M. Roks, Department of Internal Medicine, Erasmus MC, University Medical Center Rotterdam, Wytemaweg 80, Rotterdam 3015 CN, the Netherlands. E-mail: a.roks@erasmusmc.nl

How to cite this article: Jüttner AA, Mohammadi Jouabadi S, van der Linden J, de Vries R, Barnhoorn S, Garrelds IM, Goos Y, van Veghel R, van der Pluijm I, Danser AHJ, Mastroberardino PG, van der Graaf AC, Swart DH, Henning RH, Visser JA, Krenning G, Roks AJM. The modified 6-chromanol SUL-238 protects against accelerated vascular aging in vascular smooth muscle *Ercc1*-deficient mice. *J Cardiovasc Aging* 2024;4:20. https://dx.doi.org/10.20517/jca.2024.10

Received: 13 Jun 2024 **First Decision:** 6 Aug 2024 **Revised:** 20 Sep 2024 **Accepted:** 25 Sep 2024 **Published:** 14 Oct 2024

Academic Editor: Ali J. Marian **Copy Editor:** Yu-Fei Wang **Production Editor:** Yu-Fei Wang

Abstract

Introduction: Vascular aging is marked by increased mitochondrial reactive oxygen species (ROS) production, which leads to decreased nitric oxide (NO)-mediated vasodilation. Loss of NO can be partially compensated by endothelium-derived hyperpolarization (EDH), which partly relies on increased mitochondrial Ca^{2+} release to maintain vascular dilation. Thus, intervention in mitochondria may target both NO and EDH signaling to alleviate aging-related vascular dysfunction. DNA damage by mitochondrial ROS is an important cause of organismal aging. Previous work showed that local vascular *Ercc1* knockout dramatically accelerates vascular aging. The aim of the

study was to investigate the effect of chronic treatment with the modified 6-chromanol, SUL-238, an inhibitor of mitochondrial reverse electron flux and ROS, in a mouse model of accelerated vascular smooth muscle aging induced by DNA repair endonuclease *Ercc1* knockout (SMC-KO).

Aim: The aim of the study was to investigate the effect of chronic treatment with the modified 6-chromanol, SUL-238, an inhibitor of mitochondrial reverse electron flux and ROS, in a mouse model of accelerated vascular smooth muscle aging induced by DNA repair endonuclease *Ercc1* knockout (SMC-KO).

Methods: SMC-KO mice and healthy wild-type littermates received SUL-238 (90 mg/kg/day) in drinking water from 12 to 22 weeks of age. At the age of 21 weeks, arterial stiffness was measured *in vivo* with echography and they were euthanized at the age of 22 weeks. *Ex vivo* vascular function was assessed in wire myography setups and mitochondrial function of the thoracic aorta was assessed using a seahorse assay.

Results: SMC-KO mice showed reduced EDH-mediated vasodilation, elevated arterial stiffness, and increased elastin breaks at 22 weeks of age compared to their wild-type littermates. SUL-238 improved EDH, thus restoring aortic and mesenteric relaxation in SMC-KO mice. Furthermore, the number of elastin breaks was reduced and arterial stiffness normalized after treating SMC-KO mice with SUL-238. Mitochondrial respiration measured in the aorta was not different between the groups.

Conclusion: Chronic treatment with SUL-238 alleviates features of vascular aging, including decreased vasodilation and increased arterial stiffness. SUL-238 seems to have a more general effect on aging rather than involving a direct coupling between mitochondrial function and vascular signaling. SUL-238 is the first small-molecule drug reported to increase EDH after chronic treatment.

Keywords: Vascular aging, SUL-238, mitochondria, endothelium-derived hyperpolarization (EDH)

INTRODUCTION

Cardiovascular diseases are the major cause of morbidity and mortality worldwide[1]. Aging is a major intrinsic risk factor for developing cardiovascular diseases, especially those of a non-obstructive nature[2]. The latter involves the natural decline of vascular function and elasticity over time (non-atherosclerotic vascular aging), which includes decreased endothelial cell (EC) and vascular smooth muscle cell (VSMC) function[2].

One of the hallmarks of aging is mitochondrial dysfunction, in which mitochondria produce excessive amounts of free electrons, leading to reactive oxygen species (ROS) production and oxidative stress[3]. In the aging vasculature, these ROS can interact with nitric oxide (NO)-cyclic guanosine monophosphate (cGMP)-mediated signaling[4,5], which leads to decreased NO bioavailability[3,6] and causes endothelial and smooth muscle dysfunction, thrombosis, and fibrosis[4,5]. Alternatively, mitochondrial ROS can be more generally involved in vascular aging. This involvement could stem from an increase in DNA damage, although this has not yet been directly demonstrated. Such more general aging could also implicate another main vasodilator pathway, endothelium-derived hyperpolarization (EDH)[7], of which relatively little is known in the aging vasculature. EDH signals through calcium-activated potassium channels (K_{Ca}), leading to the lowering of the cell membrane potential (hyperpolarization), which results in VSMC relaxation[8]. NO and EDH signaling are carefully balanced in the healthy vasculature depending on species and vascular bed[8]. During aging, the relative contribution of these pathways to vasodilation can change and this involves both EC and VSMC.[8,9] It has been postulated that during aging, EDH signaling initially compensates for NO loss, which was demonstrated at the level of EC to maintain vasodilation[10], but is eventually lost[11,12]. This can deteriorate tonus regulation through vasomotor activity and compliance. Recently, it was shown

that EDH and mitochondrial calcium signaling are linked, and this relationship is more pronounced in the aged vasculature, partly mediated by increased mitochondrial Ca^{2+} release in the aging endothelium[10]. As a therapeutic concept to target vascular aging, improvement of both the NO- and EDH-pathway through modulation of mitochondrial function would be attractive.

The novel compound class of SUL-compounds, modified 6-chromanols, supports mitochondrial function by preventing reverse electron flux, thereby reducing ROS formation and maintaining mitochondrial ATP production in preclinical models of diabetes, ischemia-reperfusion, sepsis, and hypothermia rewarming[13-18]. Vascular function was improved by SUL-compounds in these models where increased ROS decreases endothelial NO bioactivity[13,15]. Theoretically, SUL compounds might act on NO availability during vascular aging by decreasing ROS. It is not known if they might also have a more general anti-aging effect. Moreover, their effects on aging VSMC have not been tested, presenting an important lacuna in the research field.

It has been well-established that DNA damage accumulation throughout life is a prominent cause of aging[3,4]. It has been well-established that targeting of DNA maintenance proteins, such as the endonuclease *Ercc1*, accelerates vascular aging[19-21]. *Ercc1*-defective models rapidly develop a remarkable resemblance with human non-atherosclerotic vascular aging, often more pronounced and complete than naturally aging mice, and are very suitable for intervention studies due to the short period required to develop the aging phenotype[22-25]. Even vascular-specific accelerated aging mouse models have been generated, enabling the VSMC-specific study of aging[22]. The aim of the present study is to investigate (1) the changes in VSMC mitochondrial respiration, (2) its association with vascular aging features and NO - EDH signaling, and (3) the effect of chronic treatment with SUL-238 in a mouse model of accelerated vascular smooth muscle cell aging by *Ercc1* knockout (SMC-KO mouse).

MATERIAL AND METHODS

Animals

Animals were bred as described previously[26]. In brief, the cre-loxP system was used to generate VSMC-targeted *Ercc1* KO mice by crossbreeding mice with a SM22α-promotor construct [Taglntm2(cre)Yec, C57Bl/6 background, The Jackson Laboratory, USA] with mice with the $Ercc1^{flox/-}$ construct (Ercc1tm2Dwm, FVB background, Erasmus MC colony). Mice with successful *Ercc1* KO were referred to as SMC-KO mice and their wild-type littermates (WT) were used as control mice. Male and female animals (8 per sex) were housed in groups in ventilated cages with food and water *ad libitum* and 12 h light/dark cycle. 16 SMC-KO and 16 WT were treated with SUL-238, the water-soluble hydrochloride salt of SUL-138, in drinking water (90 mg/kg/day), and the same number of animals received regular drinking water starting at the age of 12 weeks when vascular dysfunction started to develop in SMC-KO mice[22]. Blood plasma levels of SUL-238 were measured by LC-MS (by Sulfateq B.V., the Netherlands) in blood drawn during euthanization and were, on average, 205 ± 30 μg/L, similar to previous studies[27].

Animal experiments were performed at the EDC (Erasmus Laboratory Animal Science Center) following the guidelines from Directive 2010/63/EU. All studies were approved by the National Animal Care Committee and within Erasmus University Medical Center Rotterdam.

In vivo pulse wave velocity measurement

Mice were anesthetized (4% isoflurane), intubated, and connected to a pressure-controlled ventilator[28]. Anesthesia was sustained (under 2.5% isoflurane), and the body temperature was maintained at 37 °C. The stiffness of the abdominal aorta was assessed non-invasively using ultrasound (Visualsonic, USA) to derive

the local pulse wave velocity (PWV)[29]. The acquired ECG-triggered Kilohertz Visualization (EKV) images were analyzed using the VevoVasc package. This involved acquiring sequences of the longitudinal axis of the abdominal aorta, and subsequently analyzing the transmission time (ΔT) of the pulse wave along two distinct locations separated by a pre-defined distance (ΔD) in the arterial wall. The calculation of PWV was performed as ΔD/ΔT.

Laser Doppler measurements

In vivo vasodilation was measured using the Laser Doppler technique (LDPI, Perimed, PeriScan PIM 3 System), as described previously[26]. In brief, animals were anesthetized (2.8% isoflurane/O_2) and put on a heating pad to maintain the body temperature at 37 °C. After recording the baseline blood flow, the shaved hind leg was occluded for 2 min, followed by release and recording the blood flow until returning back to baseline. The results were analyzed in GraphPad Prism 8.0.1, evaluating the area under the curve (AUC) and maximal response per animal, the latter being expressed as a% difference from the recorded baseline.

Mitochondrial respiration

Mitochondrial respiration was assessed using Seahorse XF24 Islet Capture Microplates (Agilent, USA) and measured with the Seahorse XF24 Extracellular Flux Analyzer (Agilent, USA), as described previously[30]. In brief, 2 mm pieces of thoracic aorta were put in XF Assay Medium (Agilent, USA) supplemented with 1 mmol/L pyruvate, 2 mmol/L glutamine, 10 mmol/L glucose, incubated at 37 °C without CO_2 to measure the baseline respiration, followed by adding mitochondrial stress compounds sequentially: 10 µmol/L oligomycin to assess ATP-linked respiration, 1 µmol/L FCCP to estimate maximal mitochondrial respiratory capacity, and 10 µmol/L Antimycin A to evaluate non-mitochondrial respiration. These parameters were calculated with the Seahorse Wave software (version 2.6.3) as the maximal response after adding the corresponding compound, corrected for non-mitochondrial respiration and protein concentration. Proteins were isolated in homogenization buffer [0.3 mol/L sucrose, 50 mmol/L Tris-HCl pH 7.5, 1 mmol/L EDTA, 1 mmol/L EGTA, 1 mmol/L sodium-orthovanadate, 50 mmol/L sodium fluoride, 1 mmol/L DTT, 1 mmol/L PMSF, 1% (v/v) Triton x-100, phosphatase inhibitor cocktail 3 (Sigma-Aldrich), and cOmplete™ Protease Inhibitor Cocktail (Roche)] and protein concentration measured in a Lowry Assay.

Ex vivo vascular function

After euthanasia by exsanguination, thoracic aorta and the intestine were collected in cold Krebs-Henseleit buffer (118 mmol/L NaCl, 4.7 mmol/L KCl, 1.2 mmol/L $MgSO_4$, 1.2 mmol/L KH_2PO_4, 2.5 mmol/L $CaCl_2$, 11 mmol/L glucose, 25 mmol/L $NaHCO_3$, pH 7.4). Thoracic aorta and mesenteric arteries, isolated from the intestine, were mounted in wire myograph setups (DMT, Denmark) warmed at 37 °C and aerated with 95% CO_2/5% O_2. The vessel segments were then normalized by stretching them until 90% of the estimated diameter, at which the effective transmural pressure of 100 mmHg was reached, as described previously[26]. Aortic and mesenteric artery segments were pre-constricted with the thromboxane A2 analogue U46619 (10^{-8}-10^{-7} mol/L), followed by adding sodium nitroprusside (10^{-11}-10^{-4} mol/L) for endothelium-independent vasodilation, or acetylcholine (10^{-9}-10^{-5} mol/L) for endothelium-dependent vasodilation followed by 10^{-4} sodium nitroprusside to assess maximal relaxation capacity of VSMC as a correction factor. To assess the pathway contribution to endothelium-dependent vasodilation in the aorta, segments were incubated for 15 min with pathway inhibitors prior to pre-constriction: L-NAME (10^{-4} mol/L) to assess NO-contribution, apamin (10^{-7} mol/L), TRAM-34 (10^{-5} mol/L), and iberiotoxin (3×10^{-8} mol/L) to assess the role of the small, intermediate, and large-conductance calcium-activated potassium channels, respectively, and glibenclamide (10^{-6} mol/L) to assess the involvement of ATP-sensitive potassium channels.

The pathway contributions were calculated in GraphPad Prism 8.0.1 by assessing the AUC for each animal and condition separately. Relative NO and EDH contribution were calculated using the following formulas:

NO contribution [%] = $(AUC_{control}-AUC_{L\text{-}NAME})/AUC_{control}*100$ and EDH contribution [%] = $(AUCL_{NAME}-AUC_{L\text{-}NAME/apamin/TRAM34})/AUC_{control}*100$.

mRNA expression

mRNA was isolated using the TRIzol method (according to the manufacturer's instruction: Fisher Scientific) and cDNA was synthesized with the Maxima H Minus First Strand cDNA synthesis kit (ThermoFisher, USA) according to the manufacturer's instructions. qPCR was performed with the CFX Opus Real-Time PCR System (Bio-Rad) using the SYBR™ Green PCR Master Mix (Applied Biosystems™, ThermoFisher, USA) with *GAPDH* and *β-actin* as housekeeping genes, measured as duplicates per sample (1 × PCR Master Mix, 200 nmol/L forward primer, 200 nmol/L reverse primer, 10 ng cDNA). Data were analyzed with the $2^{\Delta\Delta Ct}$ method. The used primers (self-designed and ordered from IDT) are listed in Supplementary Table 1.

Protein expression

Proteins were isolated from abdominal aorta by crushing the frozen tissue with a metal tool in homogenization buffer [0.3 mol/L sucrose, 50 mmol/L Tris-HCl pH 7.5, 1 mmol/L EDTA, 1 mmol/L EGTA, 1 mmol/L sodium orthovanadate, 50 mmol/L sodium fluoride, 1 mmol/L DTT, 1 mmol/L PMSF, 1% [v/v] Triton x-100, phosphatase inhibitor cocktail 3 (Sigma-Aldrich), and cOmpleteTM Protease Inhibitor Cocktail (Roche)]. Proteins were then mixed with 1x Laemmli buffer, incubated for 10 min at 65 °C and 20 µg protein was loaded on the gels. When the required separation was reached, proteins were transferred to membranes (Trans-Blot Turbo 0.2 µm PVDF Transfer Pack, Bio-Rad) with the Trans-Blot Turbo Transfer System (Bio-Rad). Membranes were then blocked with 5% [w/v] milk or BSA for 2 h at room temperature (RT), followed by overnight incubation at 4 °C in primary antibody [GAPDH (1:10,000; 10494-1-AP, Proteintech); MMP2 (1:500, #87809, Cell Signaling), MMP9 (1:100, sc-393859, Santa-Cruz), p21 (1:200; sc-6246, Santa-Cruz), p16 (1:500; 51-1325GR, BD Pharmingen)]. On the next day, the membranes were incubated for 1 h at RT in the secondary antibody [goat anti-mouse- or goat anti-rabbit-HRP conjugate (Bio-Rad, 1:3,000)], and visualized with Clarity Western ECL substrate (Bio-Rad) following the manufacturer's instructions using an Amersham Al600. Band intensity was analyzed in Image Studio Lite (LI-COR® Biosciences) and expressed relative to GAPDH.

Immunohistochemistry

The expression of p21 and RUNX2 has been assessed in aorta. The aortas were fixed in formaldehyde, segmented, and embedded in 3% [w/v] Bacto agar. The agar blocks were dehydrated using the histokinette processor (Microm) and embedded in paraffin, followed by the preparation of 4-µm thick sections. The aorta sections were deparaffinized in xylene and rehydrated through a descending ethanol series, ending with 70% [v/v] ethanol. Slides were washed with 1x PBS/0.3% [v/v] Triton x-100 and boiled for 20 min in EDTA buffer (100 mmol/L Tris-HCl, pH 9.0, with 10 mmol/L EDTA) for the p21 staining, or citrate buffer (10 mmol/L sodium citrate, pH 6.0, with 0.05% [v/v] Tween 20) for the RUNX2 staining, to expose antigens. Endogenous peroxidase activity was blocked by incubating slides in 3% [v/v] hydrogen peroxide in methanol for 10 min, followed by blocking with 5% [v/v] normal goat serum in wash buffer for 30 min. Slides were then incubated overnight at 4 °C with the primary antibodies (p21: ab107099, 1:100 and RUNX2: ab192256, 1:100, Abcam). The next day, slides were washed and incubated with a biotinylated secondary antibody (1:200) at RT for 30 min. After washing, they were treated with an avidin-biotin complex (Vectastain Universal Elite ABC kit, Vector Laboratories) for 30 min (RT). Following a final wash step, slides were incubated with DAB chromogen (DAKO Liquid DAB substrate-chromogen system) and

counterstained with eosin. The sections were dehydrated, cleared in xylene, and mounted using Pertex mounting medium. Positive cells were manually counted and corrected for surface area.

Apoptosis assay

In situ cell death was detected with the TUNEL technology (*In situ* Cell Death Detection Kit, Fluorescein, 11684795910, Roche) according to the manufacturer's instructions. Aortic segments were fixated in 4% [v/v] formaldehyde and embedded in paraffin. For antigen retrieval, the slides were heated for 1 min in 0.1 mol/L citrate buffer (pH 6.0), followed by rapid cool down in distilled filter water at RT. For the positive control, the sample was incubated for 10 min at RT with a final concentration of 1,000 U/mL DNase I (10104159001, Roche).

Histology

Carotid arteries were fixated in 4% [v/v] formaldehyde and embedded in paraffin. To analyze collagen content, slides were stained with Sirius Red. The % red was assessed per sample in ImageJ and expressed relative to the intima-media surface (measured in the von Gieson stain). Elastin breaks were analyzed in the Gieson stain with the NDP-view2 software (Hamamatsu) and expressed relative to the intima-media surface.

Immunofluorescence

For the immunofluorescence staining in carotid arteries, slides were incubated in heated citrate buffer (pH 6.0) to retrieve antigens. After blocking with 1% [w/v] BSA and 0.5% [v/v] normal goat serum in Tris-buffered saline with 1% [v/v] Tween 20 (1x TBS-T), samples were washed with 1x TBS-T and incubated with the CD31 antibody (1:500, ab182981, Abcam) at 4 °C overnight. On the next day, samples were washed with 1x TBS-T and incubated with the secondary antibody (1:100, donkey anti-rabbit antibody, Alexa Fluor™ 488, AB_2535792). Non-specific fluorescence of the vessel was quenched with the Vector® TrueVIEW® Autofluorescence Quenching Kit (SP-8400-15, Vector Laboratories) and the samples were counterstained with DAPi. The fluorescence intensity was analyzed in ImageJ with the following formula: total fluorescence = $\text{fluorescence}_{\text{region of interest}}$ - ($\text{area}_{\text{region of interest}}$ × mean $\text{fluorescence}_{\text{background}}$), and corrected for lumen circumference, which was measured in the von Gieson stain.

Ex Vivo fluorescent imaging

Six mice per group were intravenously injected with the fluorescent probe MMP Sense680™ (Perkin Elmer) at a concentration of 2 nmol/25 g body weight 24 h prior to imaging or with the fluorescent probe Annexin-Vivo 750™ (Perkin Elmer Inc.) at a concentration of 100 µL/mouse 2 h prior to imaging. After euthanasia, the aortas were harvested and imaged using the Odyssey® CLx imaging system (LI-COR® Biosciences). Fluorescence intensity was quantified using Image Studio Lite version 5.20 (LI-COR® Biosciences), with probe intensity normalized to the area, resulting in an intensity/mm² value for each aorta. The total intensity was measured and adjusted by surface area, with SMC-KO aortas normalized to simultaneously scanned WT aortas.

Statistics

All results are expressed as mean ± standard error or geometric mean ± geometric standard deviation for mRNA expression.

Dose-response curves were analyzed using the generalized linear model (GLM) with repeated measures. Results presented in column graphs were analyzed using 2-way ANOVA with post-hoc Bonferroni's multiple comparisons test or using an unpaired *t*-test if only two groups were compared to each other (WT vehicle *vs.* SMC-KO vehicle) with $P < 0.05$.

RESULTS

We hypothesized that chronic treatment with the reverse electron flux inhibitor SUL-238 would alleviate features of vascular aging in a mouse model of accelerated VSMC aging (SMC-KO mice). These features include mitochondrial dysfunction, increased vascular stiffness, decreased vasodilation, and elevated senescence-associated secretory phenotype (SASP) factors[3,6].

The entire mitochondrial respiration curve in the thoracic aorta showed a trend of being lower in SMC-KO vehicle-treated animals compared to WT vehicle-treated mice [Figure 1A]. However, when analyzing the different parts of this curve, i.e., basal respiration, ATP-linked respiration, maximal respiration and spare respiratory capacity, there was no statistically significant difference between SMC-KO and WT vehicle-treated animals [Figure 1B-E]. The treatment with SUL-238 showed a trend of increasing mitochondrial respiration in SMC-KO mice [Figure 1A]. Nevertheless, when evaluating the individual parameters mentioned above, this trend did not reach statistical significance (2-way ANOVA) [Figure 1B-E]. Within SMC-KO, SUL-238 significantly increased maximal respiration compared to vehicle ($P < 0.05$, *t*-test, separate graph not shown).

Arterial stiffness of the abdominal aorta, measured *in vivo* by PWV, was increased in SMC-KO vehicle-treated compared to WT vehicle-treated animals and normalized after treatment with SUL-238 [Figure 2A]. An example picture of the measurement is shown in Figure 2B. Microvascular blood flow, measured with the Laser Doppler technique, was decreased in SMC-KO vehicle-treated animals compared to WT vehicle-treated mice, which is in line with previous measurements[26]. The chronic treatment with SUL-238 had no effect on microvascular blood flow in SMC-KO or WT mice [Figure 2C and D].

The stiffening of arteries during aging is associated with vascular wall remodeling[2]. We observed a trend of increased collagen deposition in carotid arteries of SMC-KO vehicle-treated mice compared to WT vehicle-treated mice, which did not reach statistical significance ($P = 0.09$) [Figure 2E]. The treatment with SUL-238 normalized the collagen content in SMC-KO mice, comparable to the WT vehicle-treated level. Moreover, we observed more elastin breaks in the carotid arteries of SMC-KO vehicle-treated compared to WT vehicle-treated mice, which were significantly reduced after the treatment with SUL-238 [Figure 2F]. Representative pictures of the Sirius Red and Von Gieson stain can be found in the supplemental material [Supplementary Figure 1A and B]. Matrix metalloproteases (MMP) are involved in elastolysis, collagen deposition, endothelial apoptosis and senescence, and their expression and activity are increased during vascular aging[31]. Nevertheless, there was no significant difference in fluorescence intensity in the aorta between the groups after injecting the mice intravenously with the fluorescently labeled probe MMP Sense680™ [Supplementary Figure 1C]. Furthermore, the protein abundance of MMP2 and MMP9 in the abdominal aorta was also not statistically significantly different between the groups [Supplementary Figure 1D, E and F].

Endothelium-dependent vasodilation in the thoracic aorta of SMC-KO vehicle-treated animals was impaired, and improved by the treatment with SUL-238 [Figure 3A]. Endothelium-independent vasodilation in the thoracic aorta of vehicle-treated SMC-KO compared to vehicle-treated WT mice was reduced, and not altered by SUL-238 treatment [Figure 3B].

Next, we evaluated the pathway contributions to vasodilation by acutely adding pathway blockers to the myograph baths. Relative pathway contribution was calculated by assessing the AUC for each animal and condition separately. Endothelium-dependent vasodilation in SMC-KO animals was mainly NO-dependent [Figure 3C and D]. The treatment with SUL-238 did not enhance NO contribution to vasodilation in SMC-

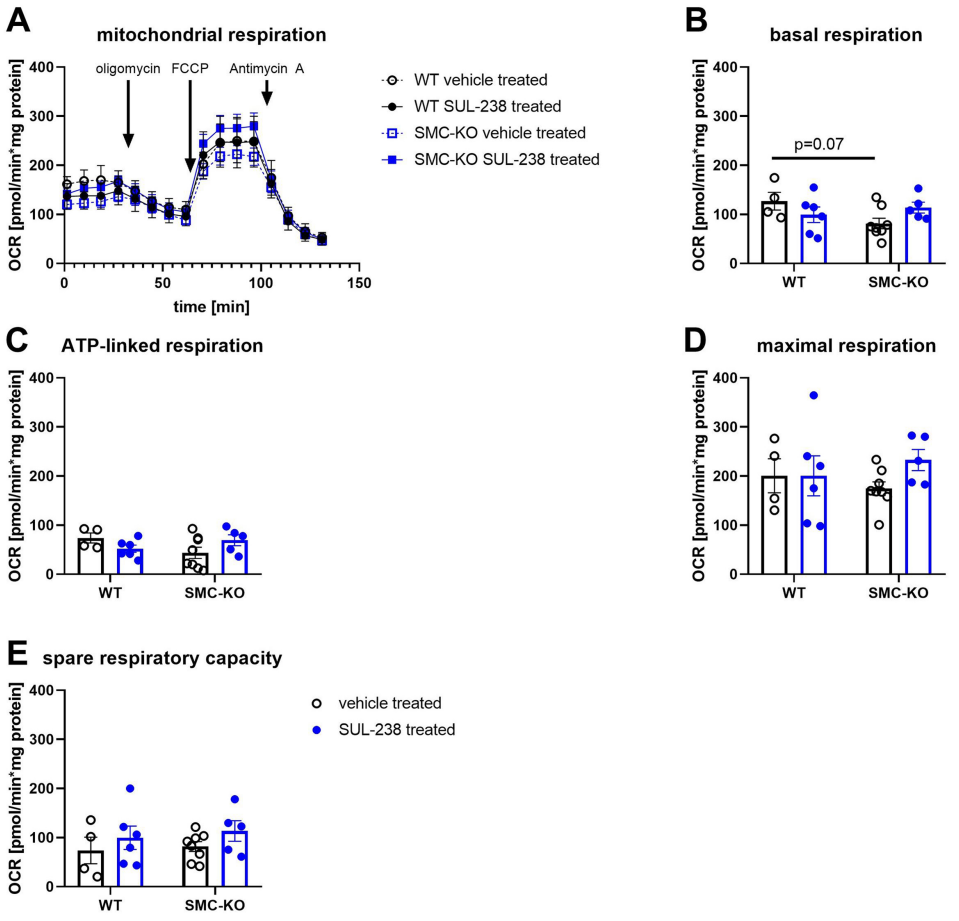

Figure 1. Mitochondrial respiration measurements in segments from thoracic aorta. OCR measurements over time (A), basal respiration (B), ATP-linked (C) and maximal respiration (D), and spare respiratory capacity (E) analyzed by 2-way ANOVA. OCR: Oxygen consumption rate; SMC-KO: DNA repair endonuclease Ercc1 knockout in vascular smooth muscle cells.

KO animals. Furthermore, we observed a left shift of the L-NAME curve for SUL-238-treated SMC-KO mice [Figure 3D]. This shift was confirmed by evaluating the logEC50, which was significantly smaller in SUL-238-treated *vs.* vehicle-treated SMC-KO mice [Figure 3E]. NO contribution in WT animals was not affected after the treatment with SUL-238 [Figure 3C and F].

EDH involves signaling through different K_{Ca} channels[32], namely small, intermediate, and large-conductance calcium-activated potassium channels (SK_{Ca}/IK_{Ca} and BK_{Ca}, respectively) as well as ATP-activated K-channel. Absolute and relative SK_{Ca}/IK_{Ca}/BK_{Ca} channel signaling almost disappeared in the SMC-KO vehicle-treated animals, but was significantly boosted after the treatment with SUL-238 [Figure 4A-C]. In WT vehicle-treated animals, EDH contribution (SK_{Ca}-/IK_{Ca} channel signaling) was slightly increased after the treatment with SUL-238, without affecting maximal vasodilation [Figure 4C and D]. BK_{Ca} channel signaling did not contribute to vasodilation in WT vehicle- or SUL-238-treated animals, and ATP-activated K-channel signaling was not involved in mediating vasodilation in either SMC-KO or WT mice (data not shown).

To assess resistance artery function, which can be used as an indicator of microcirculation dysfunction[8], endothelium-dependent vasodilation of mesenteric arteries was evaluated. Vasodilation was decreased in

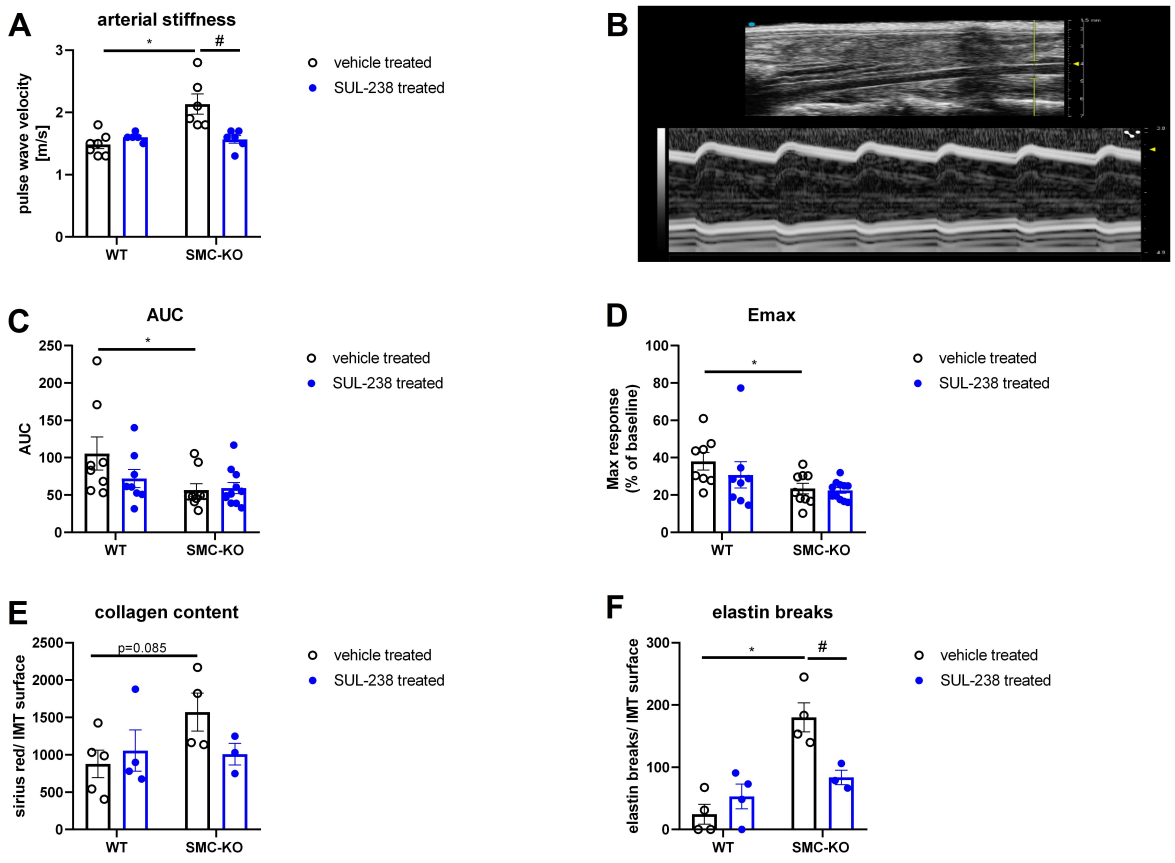

Figure 2. *In vivo* vascular function measurements. Arterial stiffness (A) and example picture of pulse wave velocity measurement in abdominal aorta (B). Laser Doppler measurements describing AUC (C) and maximal response (D). *Ex vivo* histological analysis of carotid arteries to assess collagen content (E) and elastin breaks (F). The 2-way ANOVA with *significant effect of genotype and # significant effect of SUL-238 with $P < 0.05$. AUC: Area under the curve; SMC-KO: DNA repair endonuclease Ercc1 knockout in vascular smooth muscle cells.

SMC-KO vehicle-treated compared to WT vehicle-treated mice[23], which could be rescued by treatment with SUL-238 [Figure 4E].

Mitochondrial ROS can cause decreased endothelium-dependent vasodilation on the one hand and EC cell death on the other hand[33]. We could not detect apoptotic cells in the thoracic aorta of SMC-KO or WT vehicle-treated animals analyzed with the TUNEL method [Supplementary Figure 2A]. Furthermore, there was a trend of increased apoptosis marker annexin in the aorta of SMC-KO compared to WT vehicle-treated animals, which did not reach statistical significance ($P = 0.11$) [Supplementary Figure 2B]. Lastly, we performed a CD31 staining to assess potential EC loss in the carotid arteries, but there was no statistically significant difference between the groups [Supplementary Figure 2C and D].

Next, we analyzed the expression of DNA damage and senescence markers p16 and p21. The protein abundance of p16 and p21 was slightly increased in the abdominal aorta of SMC-KO vehicle-treated animals compared to WT vehicle-treated animals [Figure 5A and B and Supplementary Figure 1F]. Because of the minor increase, there was no statistically significant effect of the treatment with SUL-238 on the expression of these markers. However, the immunohistochemical staining for p21 in the aortic arch of a separate cohort of animals indicated significantly increased numbers of p21-positive cells in SMC-KO compared to WT vehicle-treated mice [Supplementary Figure 2E]. Moreover, there were more RUNX2

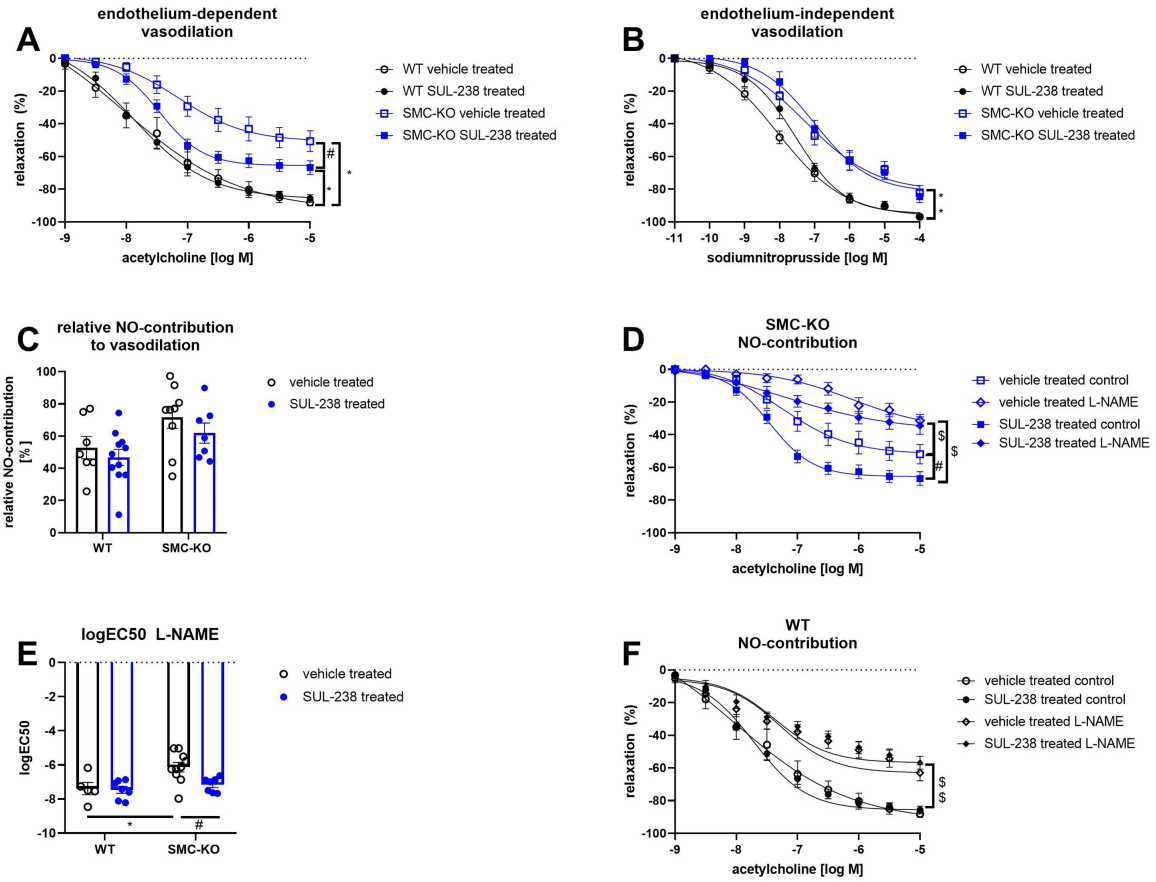

Figure 3. *Ex vivo* vascular function measured in thoracic aorta: endothelium-dependent vasodilation (A), endothelium-independent vasodilation (B), relative NO contribution to endothelium-dependent vasodilation in WT and SMC-KO animals (C), NO contribution to vasodilation in SMC-KO animals (D) and logEC50 of the curves from D (E), NO contribution in WT animals (F). Analyzed with GLM (all except for C and E) or 2-way ANOVA for C and E with *significant effect of genotype, #significant effect of SUL-238, and $significant effect of pathway inhibitor with $P < 0.05$. NO: Nitric oxide; WT: wild-type littermates; GLM: generalized linear model; SMC-KO: DNA repair endonuclease Ercc1 knockout in vascular smooth muscle cells.

positive cells, a protein that is involved in DNA-damage response[34], in the aortic arch of SMC-KO *vs.* WT vehicle-treated mice [Supplementary Figure 2F].

Inflammatory factors are elevated in SMC-KO animals in various tissues[21,26]. We confirmed upregulated mRNA expression of *il6* in the kidney of SMC-KO mice [Figure 5C]. This was accompanied by increased mRNA expression of *il1β* and *mcp1* [Figure 5D and E]. SUL-238 treatment significantly decreased *il6* and *il1β* expression in SMC-KO mice and attenuated *mcp1* mRNA expression [Figure 5C and E]. The mRNA expression levels of senescence marker *p21* and kidney injury markers *kim-1* and *ngal* were not significantly different between SMC-KO and WT vehicle-treated mice, nor were they altered after the treatment with SUL-238 [Figure 5F-H].

DISCUSSION

In this study, we investigated the effect of the chronic treatment with SUL-238, a compound that prevents reverse electron flux in mitochondria and thereby free electron spillover, in a mouse model of accelerated vascular smooth muscle cell aging (SMC-KO mice). SMC-KO mice show accelerated vascular aging features as described previously[26], with a pronounced loss of EDH response. SUL-238 restored the latter, thus

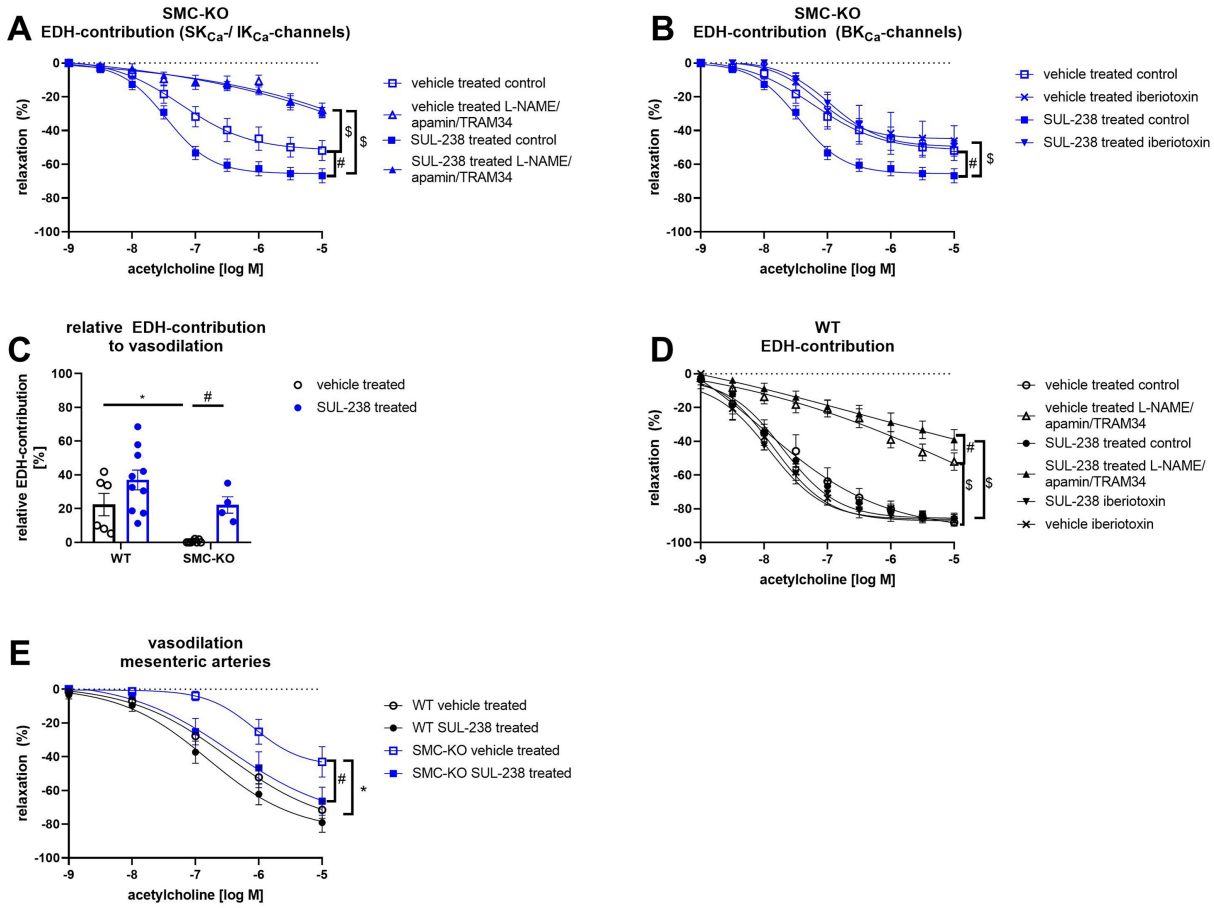

Figure 4. *Ex vivo* vascular function measured in thoracic aorta: EDH contribution in SMC-KO animals - IK_{Ca}/SK_{Ca} channels (A) and BK_{Ca} channels (B) to endothelium-dependent vasodilation, relative EDH contribution to vasodilation (C), EDH contribution in WT animals (D), and endothelium-dependent vasodilation in mesenteric arteries (E). Analyzed with GLM (all except for C) or 2-way ANOVA (C) with *significant effect of genotype, $^{\#}$significant effect of SUL-238, and $^{\$}$significant effect of inhibitor with $P < 0.05$. EDH: Endothelium-derived hyperpolarization; WT: wild-type littermates; GLM: generalized linear model; SMC-KO: DNA repair endonuclease Ercc1 knockout in vascular smooth muscle cells.

increasing aortic and mesenteric endothelium-dependent vasodilation and preventing arterial stiffening. Arterial stiffness could be linked to increased collagen deposition and elastin breaks, which were reduced after the treatment with SUL-238. Furthermore, the increased mRNA expression of inflammatory factors in the kidney of SMC-KO mice was reduced after chronic treatment with SUL-238. We excluded an effect on mitochondrial respiration[13-18] as an immediate mediator of the change in vascular signaling, because SUL-238 effects were absent in freshly harvested aortic tissue.

EDH is a main contributor to endothelium-dependent vasodilation, especially in resistance arteries[35]. EDH signaling involves different types of potassium channels which are located on EC (SK_{Ca} and IK_{Ca}-channel) or VSMC (BK_{Ca}- and ATP-activated K-channels)[8]. Loss of EDH is a feature of natural vascular aging, as demonstrated in small vessels of naturally aged rodents, and has been linked to impaired SK_{Ca}-channel function[11,12]. As explained, accumulating DNA damage is a main cause of aging, and we have now repeatedly shown that undermining *Ercc1* DNA repair function in VSMC recapitulates loss of EDH[22,23]. In mice, EDH contribution to vasodilation can be measured in aorta. Thus, a convenient model for rapid testing of EDH changes due to aging and interventions has been created by knockout of *Ercc1*. As such, we

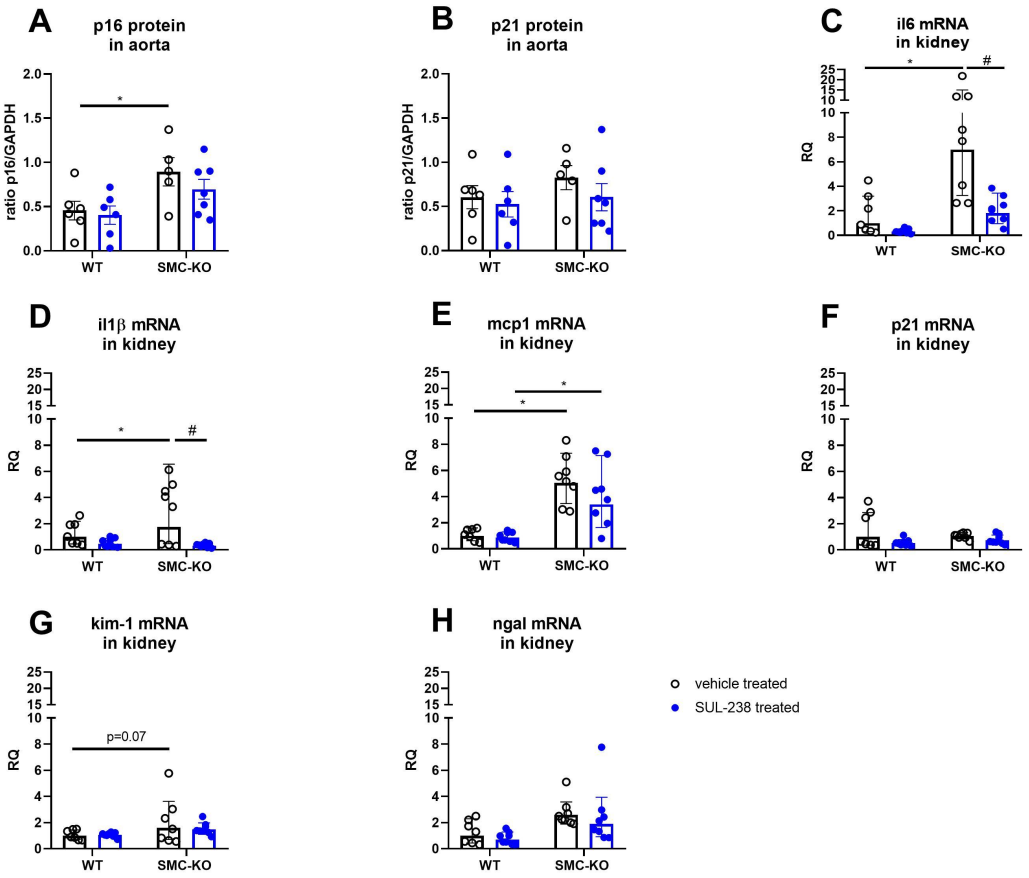

Figure 5. The p16 and p21 protein abundances in abdominal aorta (A-B). mRNA expression of SASP factors, senescence and kidney injury markers in the kidney (C-H). Analyzed with 2-way ANOVA with *significant effect of genotype and #significant effect of SUL-238 with $P < 0.05$. SMC-KO: DNA repair endonuclease Ercc1 knockout in vascular smooth muscle cells.

demonstrate that the beneficial effect of SUL-238 in SMC-KO involved both the endothelial and VSMC part of EDH signaling, as suggested by the joint implication of SK_{Ca}-/IK_{Ca}-/BK_{Ca}. This led to overall increased *ex vivo* acetylcholine vasodilation compared to SMC-KO vehicle-treated mice. In agreement, SUL-238 also restored vascular function in mesenteric arteries, as can be expected in resistance arteries.

Ercc1 knockout in fibroblasts was shown to trigger a link between cellular senescence and apoptosis, and Ercc1 knockout has occasionally been shown to induce ROS[36,37]. Theoretically, this could lead to cell death in the endothelium, and thus contribute to vasodilator dysfunction. However, we excluded the involvement of endothelial cell death in our vascular aging model, because we did not observe changes in annexin or CD31 expression and there were no TUNEL-positive cells (aorta and carotid arteries). Therefore, we also exclude the involvement of this alternative mechanism of vasomotor dysfunction.

The next question is how SUL-238 treatment preserves EDH. The non-hydrochloride form of SUL-238, SUL-138, does not directly interact with K_{Ca} channels[17]. Alternatively, being a mitochondrial drug, one might propose that SUL-238 acts on age-related changes in mitochondrial calcium-signaling that affect EDH[10]. However, the results from our parallel measurements of mitochondrial respiration and vascular function do not allude to the possibility that vasodilation and mitochondrial function are directly coupled. In contrast, *Ercc1* mutant mice have been shown to be a model to test the overall contribution of mitochondrial ROS to aging. This was demonstrated by the anti-aging effects of mitochondrial-targeted free

radical scavenger XJB-5-131 in the whole-body *Ercc1* mutant mice, *Ercc1*$^{\Delta/-}$[38]. Loss of *Ercc1* exaggerates the susceptibility of DNA to damage by ROS, and thus, even a slight reduction in mitochondrial ROS levels can have a protective effect in *Ercc1* knockout animals. *Ercc1* mutant mice spontaneously exhibit an increase in NRF2-driven anti-oxidant systems. This was suggested as a protective mechanism against the increased susceptibility to ROS[39,40]. Thus, SUL-238 is expected to display a more general anti-aging effect by mitigating ROS stress. Such action could also explain the anti-inflammatory changes in the kidney.

We chose to measure mitochondrial respiration in the aorta (seahorse assay) instead of directly measuring aortic mitochondrial ROS production (mitoSOX assay). Reliable ROS measurements should be performed in cells or isolated mitochondria from fresh tissue, but not in whole tissue or tissue homogenates[41]. Since we focused on the effects on the whole aorta, using a seahorse assay was most plausible, and this assay has been used to analyze mitochondrial respiration in aortic tissue previously[42]. However, this is a limitation of this study.

Increased vascular stiffness during aging has been linked to vascular wall remodeling, including increased collagen deposition and elastin breaks[2]. We confirmed an increase in collagens and elastin breaks in our vascular aging mouse model, which could be decreased by the treatment with SUL-238. The age-related remodeling process was linked to increased MMP expression and activity[31]. However, it has been reported that MMP regulation can either be on mRNA or on protein level, including altered protein activity[31]. Changes in protein activity cannot be detected with a regular immunoblot and could explain why we did not observe changes in protein abundance between the groups.

Moreover, vascular stiffness and impaired vasodilation during aging contribute to decreased organ perfusion[2]. The *in vivo* hyperemia test (Laser Doppler) might relate to differences in skin microvasculature and femoral artery blood flow between SMC-KO and WT vehicle-treated mice, instead of changes in aorta and mesenteric arteries, which were tested *ex vivo*. Moreover, other vasodilator pathways (NO rather than EDH) might be involved in the hyperemia measurements. The *Ercc1* KO model is a severe aging model (strongly reduced vascular function *ex vivo* and *in vivo*[22]) and the aging process might be too advanced to be fully recovered after the treatment with SUL-238. This is supported by the *ex vivo* wire myography results indicating a 50% improvement rather than full restoration upon the treatment with SUL-238. This partial improvement might not be enough to improve *in vivo* blood flow to the organs. Therefore, the question remains to what extent SUL-238 protects organs by solely improving vascular aging. The answer to this question might require a varied time schedule for analyses, evaluation of various organs, and comparisons between various cell tissue-specific accelerated aging models, requiring multiple studies.

In summary, vasodilator dysfunction and reduced compliance due to DNA damage in VSMC can be prevented by SUL-238, a mitochondrial reverse electron flux inhibitor. Preservation of EDH plays an important role in the beneficial effect on vasodilation. In all likelihood, this involved a general effect on aging rather than a direct coupling between mitochondrial function and vascular signaling. The results might have implications for the use of SUL-238 in primary prevention of vascular aging.

DECLARATIONS

Authors' contributions

Made substantial contributions to the conception and design of the study and performed data analysis and interpretation: Jüttner AA, Roks AJM, Henning RH, Krenning G

Performed data acquisition, as well as providing administrative, technical, and material support: Mohammadi Jouabadi S, de Vries R, Barnhoorn S, van der Linden J, Garrelds IM, Goos Y, van Veghel R,

van der Pluijm I, Mastroberardino PG, van der Graaf AC, Swart DH, Danser AHJ, Visser JA

Availability of data and materials

Additional data can be found in the supplementary information of this article.

Financial support and sponsorship

This work was supported by EMCLSH 19013 and Sulfateq B.V.

Conflicts of interest

Swart DH, van der Graaf AC, and Krenning G are employed at Sulfateq (Groningen, the Netherlands), a company that owns patents on SUL-138 and produces and markets this compound and similar products. All other authors declared that there are no conflicts of interest.

Ethical approval and consent to participate

All studies were approved by the National Animal Care Committee and within Erasmus University Medical Center Rotterdam [license AVD1010020209426; NTS-NL-870239: Gezondheidsproblemen veroorzaakt door vaatveroudering, en behandeling daarvan (europa.eu)].

Consent for publication

Not applicable.

REFERENCES

1. Collaborators GRF. Global, regional, and national comparative risk assessment of 79 behavioural, environmental and occupational, and metabolic risks or clusters of risks, 1990-2015: a systematic analysis for the global burden of disease study 2015. *Lancet* 2016;388:1659-724. DOI PubMed PMC
2. Jouabadi SM, Ataabadi EA, Golshiri K, et al. Clinical impact and mechanisms of non-atherosclerotic vascular aging: the new kid to be blocked. *Can J Cardiol* 2023;39:1839-58. DOI PubMed
3. López-Otín C, Blasco MA, Partridge L, Serrano M, Kroemer G. Hallmarks of aging: an expanding universe. *Cell* 2023;186:243-78. DOI PubMed
4. Bautista-Niño PK, Portilla-Fernandez E, Vaughan DE, Danser AH, Roks AJ. DNA damage: a main determinant of vascular aging. *Int J Mol Sci* 2016;17:748. DOI PubMed PMC
5. Hadi HA, Carr CS, Al Suwaidi J. Endothelial dysfunction: cardiovascular risk factors, therapy, and outcome. *Vasc Health Risk Manag* 2005;1:183-98. DOI PubMed PMC
6. Jüttner AA, Danser AHJ, Roks AJM. Pharmacological developments in antihypertensive treatment through nitric oxide-cgmp modulation. *Adv Pharmacol* 2022;94:57-94. DOI PubMed
7. Golshiri K, Ataei Ataabadi E, Portilla Fernandez EC, Jan Danser AH, Roks AJM. The importance of the nitric oxide-cgmp pathway in age-related cardiovascular disease: focus on phosphodiesterase-1 and soluble guanylate cyclase. *Basic Clin Pharmacol Toxicol* 2020;127:67-80. DOI PubMed
8. Vanhoutte PM, Shimokawa H, Feletou M, Tang EH. Endothelial dysfunction and vascular disease - a 30th anniversary update. *Acta Physiol (Oxf)* 2017;219:22-96. DOI PubMed
9. Godo S, Sawada A, Saito H, et al. Disruption of physiological balance between nitric oxide and endothelium-dependent hyperpolarization impairs cardiovascular homeostasis in mice. *Arterioscler Thromb Vasc Biol* 2016;36:97-107. DOI
10. Behringer EJ, Segal SS. Impact of aging on calcium signaling and membrane potential in endothelium of resistance arteries: a role for mitochondria. *J Gerontol A Biol Sci Med Sci* 2017;72:1627-37. DOI PubMed PMC
11. Kong BW, Man RY, Gao Y, Vanhoutte PM, Leung SW. Reduced activity of skc a and na-k atpase underlies the accelerated impairment of edh-type relaxations in mesenteric arteries of aging spontaneously hypertensive rats. *Pharmacol Res Perspect* 2015;3:e00150. DOI PubMed PMC
12. Chennupati R, Lamers WH, Koehler SE, De Mey JGR. Endothelium-dependent hyperpolarization-related relaxations diminish with age in murine saphenous arteries of both sexes. *Br J Pharmacol* 2013;169:1486-99. DOI PubMed PMC
13. Star BS, van der Slikke EC, van Buiten A, Henning RH, Bouma HR. The novel compound sul-138 counteracts endothelial cell and kidney dysfunction in sepsis by preserving mitochondrial function. *Int J Mol Sci* 2023;24:6330. DOI PubMed PMC

14. Hajmousa G, Vogelaar P, Brouwer LA, van der Graaf AC, Henning RH, Krenning G. The 6-chromanol derivate sul-109 enables prolonged hypothermic storage of adipose tissue-derived stem cells. *Biomaterials* 2017;119:43-52. DOI PubMed
15. Lambooy SPH, Bidadkosh A, Nakladal D, et al. The novel compound sul-121 preserves endothelial function and inhibits progression of kidney damage in type 2 diabetes mellitus in mice. *Sci Rep* 2017;7:11165. DOI PubMed PMC
16. Vogelaar PC, Roorda M, de Vrij EL, et al. The 6-hydroxychromanol derivative sul-109 ameliorates renal injury after deep hypothermia and rewarming in rats. *Nephrol Dial Transplant* 2018;33:2128-38. DOI
17. Vogelaar PC, Nakladal D, Swart DH, et al. Towards prevention of ischemia-reperfusion kidney injury: pre-clinical evaluation of 6-chromanol derivatives and the lead compound sul-138. *Eur J Pharm Sci* 2022;168:106033. DOI PubMed
18. Han B, Poppinga WJ, Zuo H, et al. The novel compound sul-121 inhibits airway inflammation and hyperresponsiveness in experimental models of chronic obstructive pulmonary disease. *Sci Rep* 2016;6:26928. DOI PubMed PMC
19. Durik M, Kavousi M, van der Pluijm I, et al. Nucleotide excision DNA repair is associated with age-related vascular dysfunction. *Circulation* 2012;126:468-78. DOI PubMed PMC
20. Weeda G, Donker I, de Wit J, et al. Disruption of mouse ercc1 results in a novel repair syndrome with growth failure, nuclear abnormalities and senescence. *Curr Biol* 1997;7:427-39. DOI
21. Yousefzadeh MJ, Zhao J, Bukata C, et al. Tissue specificity of senescent cell accumulation during physiologic and accelerated aging of mice. *Aging Cell* 2020;19:e13094. DOI PubMed PMC
22. Ataei Ataabadi E, Golshiri K, van der Linden J, et al. Vascular ageing features caused by selective DNA damage in smooth muscle cell. *Oxid Med Cell Longev* 2021;2021:2308317. DOI PubMed PMC
23. Golshiri K, Ataabadi EA, Jüttner AA, et al. The effects of acute and chronic selective phosphodiesterase 1 inhibition on smooth muscle cell-associated aging features. *Front Pharmacol* 2021;12:818355. DOI PubMed PMC
24. Bautista-Niño PK, Portilla-Fernandez E, Rubio-Beltrán E, et al. Local endothelial DNA repair deficiency causes aging-resembling endothelial-specific dysfunction. *Clin Sci (Lond)* 2020;134:727-46. DOI
25. van der Linden J, Stefens SJM, Heredia-Genestar JM, et al. Ercc1 DNA repair deficiency results in vascular aging characterized by vsmc phenotype switching, ecm remodeling, and an increased stress response. *Aging Cell* 2024;23:e14126. DOI PubMed PMC
26. Ataei Ataabadi EGK, van der Linden J, Jüttner A, et al. Vascular ageing features caused by selective DNA damage in smooth muscle cell. *Oxid Med Cell Longev* 2024:2308317. DOI PubMed PMC
27. de Veij Mestdagh CF, Koopmans F, Breiter JC, et al. The hibernation-derived compound sul-138 shifts the mitochondrial proteome towards fatty acid metabolism and prevents cognitive decline and amyloid plaque formation in an alzheimer's disease mouse model. *Alzheimers Res Ther* 2022;14:183. DOI PubMed PMC
28. de Waard MC, van der Velden J, Bito V, et al. Early exercise training normalizes myofilament function and attenuates left ventricular pump dysfunction in mice with a large myocardial infarction. *Circ Res* 2007;100:1079-88. DOI
29. Sharma N, Sun Z, Hill MA, Hans CP. Measurement of pulse propagation velocity, distensibility and strain in an abdominal aortic aneurysm mouse model. *J Vis Exp* 2020;23:156. DOI PubMed PMC
30. Milanese C, Bombardieri CR, Sepe S, et al. DNA damage and transcription stress cause atp-mediated redesign of metabolism and potentiation of anti-oxidant buffering. *Nat Commun* 2019;10:4887. DOI PubMed PMC
31. Wang M, Kim SH, Monticone RE, Lakatta EG. Matrix metalloproteinases promote arterial remodeling in aging, hypertension, and atherosclerosis. *Hypertension* 2015;65:698-703. DOI PubMed PMC
32. Leung SW, Vanhoutte PM. Endothelium-dependent hyperpolarization: age, gender and blood pressure, do they matter? *Acta Physiol (Oxf)* 2017;219:108-23. DOI PubMed
33. Mikhed Y, Daiber A, Steven S. Mitochondrial oxidative stress, mitochondrial DNA damage and their role in age-related vascular dysfunction. *Int J Mol Sci* 2015;16:15918-53. DOI PubMed PMC
34. Cobb AM, Yusoff S, Hayward R, et al. Runx2 (runt-related transcription factor 2) links the DNA damage response to osteogenic reprogramming and apoptosis of vascular smooth muscle cells. *Arterioscler Thromb Vasc Biol* 2021;41:1339-57. DOI
35. Brandes RP, Schmitz-Winnenthal FH, Félétou M, et al. An endothelium-derived hyperpolarizing factor distinct from no and prostacyclin is a major endothelium-dependent vasodilator in resistance vessels of wild-type and endothelial no synthase knockout mice. *Proc Natl Acad Sci U S A* 2000;97:9747-52. DOI PubMed PMC
36. Kim DE, Dollé MET, Vermeij WP, et al. Deficiency in the DNA repair protein ercc1 triggers a link between senescence and apoptosis in human fibroblasts and mouse skin. *Aging Cell* 2020;19:e13072. DOI PubMed PMC
37. Czerwińska J, Nowak M, Wojtczak P, et al. Ercc1-deficient cells and mice are hypersensitive to lipid peroxidation. *Free Radic Biol Med* 2018;124:79-96. DOI PubMed PMC
38. Robinson AR, Yousefzadeh MJ, Rozgaja TA, et al. Spontaneous DNA damage to the nuclear genome promotes senescence, redox imbalance and aging. *Redox Biol* 2018;17:259-73. DOI PubMed PMC
39. Vermeij WP, Dollé ME, Reiling E, et al. Restricted diet delays accelerated ageing and genomic stress in DNA-repair-deficient mice. *Nature* 2016;537:427-31. DOI PubMed PMC
40. Ataei Ataabadi E, Golshiri K, Jüttner AA, et al. Soluble guanylate cyclase activator bay 54-6544 improves vasomotor function and survival in an accelerated ageing mouse model. *Aging Cell* 2022;21:e13683. DOI PubMed PMC
41. Murphy MP, Bayir H, Belousov V, et al. Guidelines for measuring reactive oxygen species and oxidative damage in cells and in vivo. *Nat Metab* 2022;4:651-62. DOI PubMed PMC
42. Karaś A, Bar A, Pandian K, et al. Functional deterioration of vascular mitochondrial and glycolytic capacity in the aortic rings of aged

mice. *Geroscience* 2024;46:3831-44. DOI PubMed PMC